

Properties of D-mesons in nuclear matter within a self-consistent coupled-channel approach

L. Tolós, J. Schaffner-Bielich, A. Mishra

Institut für Theoretische Physik J.W. Goethe Universität, Frankfurt am Main

(July 19, 2018)

Abstract

The spectral density of the D -meson in the nuclear environment is studied within a self-consistent coupled-channel approach assuming a separable potential for the bare meson-baryon interaction. The DN interaction, described through a G-matrix, generates dynamically the $\Lambda_c(2593)$ resonance. This resonance is the charm counterpart of the $\Lambda(1405)$ resonance generated from the s-wave $\bar{K}N$ interaction in the $I=0$ channel. The medium modification of the D -meson spectral density due to the Pauli blocking of intermediate states as well as due to the dressing of the D -mesons, nucleons and pions is investigated. We observe that the inclusion of coupled-channel effects and the self-consistent dressing of the D -meson results in an overall reduction of the in-medium D -meson changes compared to previous work which neglect those effects.

PACS: 14.40.Lb, 14.20.Gk, 21.65.+f

Keywords: DN interaction, $\Lambda_c(2593)$ resonance, coupled-channel self-consistent calculation, D -meson spectral density, hadrons in the medium.

I. INTRODUCTION

The study of the properties of hadrons in a hot and dense medium is an important problem in strong interaction physics. It is a topic of active research interest as it has direct implications in heavy-ion collision experiments, as well as in the study of astrophysical compact objects like neutron stars. The medium modifications of hadrons are probed in the relativistic heavy-ion collision experiments. In particular, at CERN-SPS, the experimentally observed dilepton spectra [1,2] have been attributed to the medium modifications of the spectral properties of the vector mesons, especially of the ρ -meson [3–7] and can not be explained by the vacuum hadronic properties. Furthermore, the K^\pm production from nuclear collisions at GSI-SIS energies of 1-2 AGeV have shown that in-medium properties of the kaons have been seen in the collective flow pattern of K^+ mesons as well as in the abundancy and spectra of antikaons [4,8–15]. The medium modifications of $D(\bar{D})$ mesons, which show analogy to the $\bar{K}(K)$ mesons resulting from replacing s-quark (s-antiquark) by the c-quark (c-antiquark), have also become a subject of recent interest [16–21]. The medium changes

for D -mesons can have important consequences for the open charm enhancement in nucleus-nucleus collisions [22] as well as for J/Ψ suppression as observed at the SPS [23]. The NA50 Collaboration has claimed to see an open charm enhancement by up to a factor of three in central $Pb + Pb$ collisions at 158 A·GeV [24]. The medium modifications of the open charm mesons ($D(\bar{D})$) can also modify the high mass ($M > 2 \text{ GeV}$) dilepton spectra [25] since they can be produced abundantly in high energy heavy-ion collisions. Transverse momentum spectra of electrons from $Au + Au$ collisions at $\sqrt{s} = 130 \text{ GeV}$ have been measured at midrapidity by the PHENIX experiment at RHIC [26]. The spectra show an excess above the background from decays of light hadrons and photon conversion. The observed signal is consistent with that expected from semi-leptonic decays of charmed mesons.

In high energy heavy-ion collisions at RHIC ($\sqrt{s} \sim 200 \text{ GeV}$), an appreciable contribution of J/Ψ suppression is expected to be due to the formation of a quark-gluon Plasma (QGP) [27]. However, the medium modification of D -mesons should modify the J/Ψ absorption in hot and dense nuclear medium and can provide a possible explanation for J/Ψ suppression. The effect of the hadron absorption of J/Ψ 's is found to be not negligible [28–30]. It is thus of importance to understand the interactions of the D -mesons in the hadronic medium for J/Ψ production as well.

At finite densities, the medium modification of the D -meson mass has been studied using the QCD sum rule (QSR) approach [16,19]. Due to the presence of a light quark in the D -meson, the mass modification of the D -meson has a large contribution from the light quark condensates. The large shift of mass ($\simeq 50 \text{ MeV}$ at nuclear matter density, ρ_0) in the D -mesons is originated from the contribution of the $m_c \langle \bar{q}q \rangle_N$ term in the operator product expansion. The quark-meson coupling (QMC) model predicts a mass drop of the D -meson to be of the order of 60 MeV at $\rho = \rho_0$ [21], which is very similar to the value obtained in the QCD sum rule calculations of Refs. [16,19]. At finite temperatures, the studies of quarkonium dissociation [20,31] using heavy quark potential from lattice QCD [32] suggest a similar drop of the D -meson mass.

In a recent work, the mass modification of the D -meson in hot and dense matter, arising due to its interaction with the light hadron sector, was studied in a chiral effective model [33]. The chiral SU(3) model, used to study the hadronic properties in the hot hyperonic matter [34] was generalized to SU(4) to include the charmed mesons. Interactions of the D -meson with the light hadron sector were derived to study the in-medium mass of the D -meson.

In all these investigations, the spectral features of a D -meson embedded in hot and dense matter have not been studied. Coupled-channel effects as well as dressing of intermediate propagators have been completely ignored, which turned out to be crucial for describing the strange counter part of the D -meson, the \bar{K} meson in the nuclear medium. In the present investigation, the spectral density for the D -meson is calculated using a self-consistent coupled-channel G-matrix calculation. The medium effects like the Pauli blocking on the nucleons in the intermediate states and the effects from the dressing of the D -mesons, nucleons as well as pions are investigated. The coupled-channel formalism generates dynamically the $\Lambda_c(2593)$ resonance, like the $\Lambda(1405)$ resonance for the case of antikaons.

We have organized the present paper as follows. In Sect. II we first review our formalism. Our results are presented and discussed in Sect. III and the concluding remarks are given in Sect. IV.

II. FORMALISM

In this section we present the formalism to obtain the self-energy or single-particle potential of a D-meson embedded in infinite symmetric nuclear matter. This self-energy accounts for the interaction of the D-meson with the nucleons and its calculation requires the knowledge of the in-medium DN interaction, which will be described by a G -matrix. The medium effects incorporated in this G -matrix include the Pauli blocking on the nucleons in the intermediate states as well as the dressing of the D-meson, nucleons and pions.

A. In-medium s-wave DN interaction

The effective DN interaction in the nuclear medium or G -matrix is obtained from the bare DN interaction, in a similar way as done in Ref. [35] for the $\bar{K}N$ interaction. However, in this case, only the in-medium s-wave DN interaction is considered taking, as a bare interaction, a separable potential model as done for the K^-p interaction in Ref. [36]. For the separable potential we use the following ansatz in momentum space

$$\begin{aligned} V_{i,j}(k, k') &= g^2 C_{i,j} v_i(k) v_j(k') \\ &= \frac{g^2}{\Lambda^2} C_{i,j} \Theta(\Lambda - k) \Theta(\Lambda - k') , \end{aligned} \quad (1)$$

where g is the coupling constant and Λ the cutoff. These two parameters will be determined by fixing the position and the width of the $\Lambda_c(2593)$ resonance, the analogous to the $\Lambda(1405)$ resonance in the charm sector. For the interaction matrix C_{ij} , we use the standard result derived from SU(3) flavor symmetry ([36,37]). This bare interaction allows for the transition from DN to other channels, namely, $\pi\Lambda_c$, $\pi\Sigma_c$, $\eta\Lambda_c$ and $\eta\Sigma_c$, all having charm $c = 1$. Therefore, we are confronted with a coupled-channel problem. In principle, one should use SU(4) symmetry as we incorporate charmed mesons. However, channels with a strange and charm quarks such as $K\Xi_c$, $D_s\Lambda$ or $D_s\Sigma$ have not been considered due to the fact that their respective masses are well above the DN threshold (see Fig. 1). Therefore, we only consider channels with up, down and charm-quark content keeping the SU(3) symmetry.

The resultant meson-baryon G -matrices can be grouped in a matrix notation, where each box corresponds to one channel. The DN channel can have isospin $I = 0$ or $I = 1$. In the first case, it couples to the $\pi\Sigma_c$ and $\eta\Lambda_c$ channels and the corresponding matrix has the following structure

$$\begin{pmatrix} G_{DN \rightarrow DN} & G_{\pi\Sigma_c \rightarrow DN} & G_{\eta\Lambda_c \rightarrow DN} \\ G_{DN \rightarrow \pi\Sigma_c} & G_{\pi\Sigma_c \rightarrow \pi\Sigma_c} & G_{\eta\Lambda_c \rightarrow \pi\Sigma_c} \\ G_{DN \rightarrow \eta\Lambda_c} & G_{\pi\Sigma_c \rightarrow \eta\Lambda_c} & G_{\eta\Lambda_c \rightarrow \eta\Lambda_c} \end{pmatrix} ,$$

while for $I = 1$ it can couple to the $\pi\Lambda_c$, $\pi\Sigma_c$ and $\eta\Sigma_c$ channels

$$\begin{pmatrix} G_{DN \rightarrow DN} & G_{\pi\Lambda_c \rightarrow DN} & G_{\pi\Sigma_c \rightarrow DN} & G_{\eta\Sigma_c \rightarrow DN} \\ G_{DN \rightarrow \pi\Lambda_c} & G_{\pi\Lambda_c \rightarrow \pi\Lambda_c} & G_{\pi\Sigma_c \rightarrow \pi\Lambda_c} & G_{\eta\Sigma_c \rightarrow \pi\Lambda_c} \\ G_{DN \rightarrow \pi\Sigma_c} & G_{\pi\Lambda_c \rightarrow \pi\Sigma_c} & G_{\pi\Sigma_c \rightarrow \pi\Sigma_c} & G_{\eta\Sigma_c \rightarrow \pi\Sigma_c} \\ G_{DN \rightarrow \eta\Sigma_c} & G_{\pi\Lambda_c \rightarrow \eta\Sigma_c} & G_{\pi\Sigma_c \rightarrow \eta\Sigma_c} & G_{\eta\Sigma_c \rightarrow \eta\Sigma_c} \end{pmatrix} .$$

Keeping this structure in mind, the G -matrix is formally given by

$$\begin{aligned} \langle M_1 B_1 | G(\Omega) | M_2 B_2 \rangle &= \langle M_1 B_1 | V | M_2 B_2 \rangle \\ &+ \sum_{M_3 B_3} \langle M_1 B_1 | V | M_3 B_3 \rangle \frac{Q_{M_3 B_3}}{\Omega - E_{M_3} - E_{B_3} + i\eta} \langle M_3 B_3 | G(\Omega) | M_2 B_2 \rangle . \end{aligned} \quad (2)$$

In Eq. (2), M_i and B_i represent the possible mesons (D , π , η) and baryons (N , Λ_c , Σ_c) respectively, and their corresponding quantum numbers such as spin, isospin, charm, and linear momentum. The function $Q_{M_3 B_3}$ stands for the Pauli operator which allows only intermediate nucleon states compatible with the Pauli principle. The energy variable Ω is the so-called starting energy while \sqrt{s} is the invariant center-of-mass energy, i.e., $\sqrt{s} = \sqrt{\Omega^2 - \vec{P}^2}$, where (Ω, \vec{P}) is the total meson-baryon four momentum in a frame in which nuclear matter is at rest.

The former equation for the G -matrix has to be considered together with a prescription for the single-particle energies of all the mesons and baryons participating in the reaction and in the intermediate states. These energies can be written as

$$E_{M_i(B_i)}(k) = \sqrt{k^2 + m_{M_i(B_i)}^2} + U_{M_i(B_i)}(k, E_{M_i(B_i)}^{qp}) , \quad (3)$$

where $U_{M_i(B_i)}$ is the single-particle potential of each meson (baryon) calculated at the real quasiparticle energy $E_{M_i(B_i)}^{qp}$. For baryons, this quasiparticle-energy is given by

$$E_{B_i}^{qp}(k) = \sqrt{k^2 + m_{B_i}^2} + \text{Re } U_{B_i}(k, E_{B_i}^{qp}) , \quad (4)$$

while, for mesons, it is obtained by solving the following equation

$$(E_{M_i}^{qp}(k))^2 = k^2 + m_{M_i}^2 + \text{Re } \Pi_{M_i}(k, E_{M_i}^{qp}) . \quad (5)$$

In the present paper we have considered the single-particle potential for the D -meson, nucleons and pions together with the decay width of the Σ_c meson. The reason for the inclusion of this width will be clarified in the results section.

For nucleons, as done in Ref. [38], we have used a relativistic $\sigma - \omega$ model, where the scalar and vector coupling constants, g_s and g_v respectively, are density dependent [39].

One of the most important modifications comes from the introduction of the pion self-energy, $\Pi_\pi(k, \omega)$, in the intermediate $\pi\Lambda_c$ and $\pi\Sigma_c$ states present in the construction of the effective DN interaction. The pion is dressed with the momentum and energy-dependent self-energy [40] which was also studied in Ref. [38]. This self-energy incorporates a p-wave piece built up from the coupling to $1p - 1h$, $1\Delta - 1h$ and $2p - 2h$ excitations, together with short-range correlations. The model also contains a small and constant s-wave part.

The D -meson single-particle potential in the Brueckner-Hartree-Fock approach is schematically given by

$$U_D(k, E_D^{qp}) = \sum_{N \leq F} \langle DN | G_{DN \rightarrow DN}(\Omega = E_N^{qp} + E_D^{qp}) | DN \rangle , \quad (6)$$

where the summation over nucleon states is limited by the nucleon Fermi momentum. As it can be easily seen from Eq. (6), since the effective DN interaction (G -matrix) depends

on the D -meson single-particle energy, which in turn depends on the D -meson potential, we are confronted with a self-consistent problem. We also note that the G -matrix in the above equation becomes complex due to the possibility of DN state decaying into the $\pi\Lambda_c$ and $\pi\Sigma_c$ channels. As a consequence, the potential U_D is also a complex quantity. Further details are given in the next section.

The G -matrix equation for the s-wave in-medium DN interaction in the partial wave basis using the quantum numbers of the relative and center-of-mass motion reads

$$\begin{aligned}
& \langle (M_1 B_1); k'' | G^I(P, \Omega) | (M_2 B_2); k \rangle = \langle (M_1 B_1); k'' | V^I | (M_2 B_2); k \rangle \\
& + \sum_{M_3 B_3} \int \frac{k'^2}{2\pi^2} dk' \langle (M_1 B_1); k'' | V^I | (M_3 B_3); k' \rangle \\
& \times \frac{\overline{Q}_{M_3 B_3}(k', P)}{\Omega - \sqrt{m_{B_3}^2 + \widetilde{k}_{B_3}^2} - \sqrt{m_{M_3}^2 + \widetilde{k}_{M_3}^2} - U_{B_3}(\widetilde{k}_{B_3}^2) - U_{M_3}(\widetilde{k}_{M_3}^2) + i\eta} \\
& \times \langle (M_3 B_3); k' | G^I(P, \Omega) | (M_2 B_2); k \rangle, \tag{7}
\end{aligned}$$

where the variables k , k' , k'' are the relative momenta and P is the linear center-of-mass momentum. The functions \widetilde{k}_B^2 and \widetilde{k}_M^2 are, respectively, the square of the momentum of the baryon and that of the meson in the intermediate states, averaged over the angle between the total momentum \vec{P} and the relative momentum \vec{k}' (see appendix A in Ref. [35])

$$\begin{aligned}
\widetilde{k}_B^2(k', P) &= k'^2 + \left(\frac{m_B}{m_M + m_B} \right)^2 P^2, \\
\widetilde{k}_M^2(k', P) &= k'^2 + \left(\frac{m_M}{m_M + m_B} \right)^2 P^2. \tag{8}
\end{aligned}$$

The angle average of the Pauli operator, $\overline{Q}_{M_3 B_3}(k', P)$, differs from unity only for the DN channel (for details see appendix A in Ref. [35]).

B. D -meson single-particle energy in the Brueckner-Hartree-Fock approximation

For the s-wave component of the DN interaction, the Brueckner-Hartree-Fock approximation to the single-particle potential of a D -meson embedded in a Fermi sea of nucleons [Eq. (6)] becomes

$$\begin{aligned}
U_D(k_D, E_D^{qp}(k_D)) &= \frac{1}{2\pi^2} \sum_I (2I+1)(1+\xi)^3 \int_0^{k_{max}} k^2 dk f(k, k_D) \\
&\times \langle (DN); k | G^I(\overline{P}^2, E_D^{qp}(k_D) + E_N^{qp}(\overline{k}_N^2)) | (DN); k \rangle, \tag{9}
\end{aligned}$$

where \overline{P}^2 and \overline{k}_N^2 are the square of the center-of-mass momentum and nucleon momentum, respectively, averaged over the angle between the external D -meson momentum in the lab system, \vec{k}_D , and the DN relative momentum, \vec{k} , used as integration variable in Eq. (9) (see appendix B in Ref. [35]). These angle averages eliminate the angular dependence of the G -matrix and allow to perform the angular integration in Eq. (9) analytically, giving rise to the weight function, $f(k, k_D)$,

$$f(k, k_D) = \begin{cases} 1 & \text{for } k \leq \frac{k_F - \xi k_D}{1 + \xi}, \\ 0 & \text{for } |\xi k_D - (1 + \xi)k| > k_F, \\ \frac{k_F^2 - [\xi k_D - (1 + \xi)k]^2}{4\xi(1 + \xi)k_D k} & \text{otherwise,} \end{cases} \quad (10)$$

where $\xi = \frac{m_N}{m_D}$ and k_F is the Fermi momentum. The magnitude of the relative momentum k is constrained by

$$k_{max} = \frac{k_F + \xi k_D}{1 + \xi}. \quad (11)$$

After self-consistency for the on-shell value $U_D(k_D, E_D^{qp})$ is achieved, one can obtain the complete energy dependence of the self-energy $\Pi_D(k_D, \omega)$,

$$\Pi_D(k_D, \omega) = 2\sqrt{k_D^2 + m_D^2} U_D(k_D, \omega) \quad (12)$$

by replacing E_D^{qp} in Eq. (9) by ω . This self-energy can then be used to determine the D -meson single-particle propagator in the medium,

$$D_D(k_D, \omega) = \frac{1}{\omega^2 - k_D^2 - m_D^2 - 2\sqrt{m_D^2 + k_D^2} U_D(k_D, \omega)}, \quad (13)$$

and the corresponding spectral density

$$S_D(k_D, \omega) = -\frac{1}{\pi} \text{Im } D_D(k_D, \omega). \quad (14)$$

In fact, only the value of the potential U_D at the quasiparticle energy $\omega = E_D^{qp}$ is determined self-consistently. This amounts to taking, in the subsequent iterations leading to self-consistency, the so-called ‘‘quasiparticle’’ approximation to the D -meson propagator

$$D_D^{qp}(k_D, \omega) = \frac{1}{\omega^2 - k_D^2 - m_D^2 - 2\sqrt{m_D^2 + k_D^2} U_D(k_D, E_D^{qp})}, \quad (15)$$

which gives rise to a simplified spectral strength

$$S_D^{qp}(k_D, \omega) = \frac{1}{\pi} \frac{2\sqrt{m_D^2 + k_D^2} \text{Im } U_D(k_D, E_D^{qp})}{|\omega^2 - k_D^2 - m_D^2 - 2\sqrt{m_D^2 + k_D^2} \text{Re } U_D(k_D, E_D^{qp})|^2 + |2\sqrt{m_D^2 + k_D^2} \text{Im } U_D(k_D, E_D^{qp})|^2}. \quad (16)$$

The location and width of the peak in this distribution are determined, respectively, by the real and imaginary parts of $U_D(k_D, E_D^{qp})$.

This self-consistent scheme was also used in previous works for the \bar{K} meson [35,38] and, although it represents a simplification with respect to the more sophisticated scheme followed in Refs. [41,42] for the \bar{K} case where the full energy dependence of the \bar{K} self-energy is self-consistent determined, the approximation is sufficiently good as already shown in Refs. [35,38].

III. RESULTS

We start this section by showing the mass distribution of the $\pi\Sigma_c$ state in Fig. 2. The mass distribution is given by

$$\frac{d\sigma}{dm} = C | T_{\pi\Sigma_c \rightarrow \pi\Sigma_c}^{I=0} |^2 p_{CM} \quad (17)$$

where C is related to the particular reaction generating the $\pi\Sigma_c$ state prior to final state interactions, p_{CM} is the $\pi\Sigma_c$ relative momentum and $T_{\pi\Sigma_c \rightarrow \pi\Sigma_c}^{I=0}$ is the isospin zero component of the on-shell s -wave T-matrix for the $\pi\Sigma_c$ channel. The study of the mass distribution of the $\pi\Sigma_c$ state in the $I = 0$ channel reflects the $\Lambda_c(2593)$ resonance as seen in Fig. 2. In this figure the mass distribution of the $\pi\Sigma_c$ state for $I = 0$ is displayed as a function of the C.M. energy for different sets of coupling constants g and cutoffs Λ . We observe that our coupled-channel calculation generates dynamically the $\Lambda_c(2593)$ resonance. The position (2593.9 ± 2 MeV) and width ($\Gamma = 3.6_{-1.3}^{+2.0}$ MeV) are obtained for a given set of coupling constants and cutoffs in the range between 0.8 and 1.4 GeV. This resonance was also obtained in the framework of the χ -BS(3) approach based on the chiral SU(3) Lagrangian and formulated in terms of the Bethe-Salpeter equation [43]. It is interesting to observe that the set of coupling constants and cutoffs that generate the resonance are very similar to the ones used in the $s = -1$ sector to reproduce dynamically the $\Lambda(1405)$ resonance [36].

Once the position and width of the $\Lambda_c(2593)$ resonance are reproduced dynamically, we study the effect of the different medium modifications on the resonance. The real and imaginary parts of the resulting in-medium s -wave DN amplitudes in the $I = 0$ channel for $\Lambda = 1.0$ GeV and $g^2=13.4$ and for a total momentum $|\vec{k}_D + \vec{k}_N| = 0$ are given in Fig. 3 as a function of the invariant center-of-mass energy for different approaches: T-matrix calculation (dotted lines), including Pauli blocking (dot-dashed lines) and self-consistent calculation for the D -meson (solid lines) at nuclear matter saturation density $\rho_0 = 0.17 \text{ fm}^{-3}$. Due to the fact that the resonance lies just few MeV above the $\pi\Sigma_c$ threshold, we have included the decay width of the Σ_c baryon in our calculations by considering the corresponding imaginary part for the Σ_c self-energy. In this way, the resonance is reproduced in a more realistic way, even below the $\pi\Sigma_c$ state. We clearly see, as noticed already for the $\Lambda(1405)$ resonance, the repulsive effect of the Pauli blocking on the resonance, being generated at higher energies. However, as already pointed out for the $\bar{K}N$ interaction, the shift in energy of the $\Lambda_c(2593)$ resonance is intimately connected with the energy dependence of the DN interaction and changes are expected from a self-consistent incorporation of the D -meson properties in the DN interaction. Therefore, the effect of dressing the D -meson with the complete complex self-energy on the in-medium DN amplitude makes the resonance peak stay pretty close or even at lower energies than its free space location. This is due to the attraction felt by the D -meson that compensates the repulsive effect induced by Pauli blocking on the nucleon, as already seen for the $\Lambda(1405)$ resonance in Refs. [35,36,41,42,44]. On the other hand, the real and imaginary parts of the DN amplitude become much smoother because of the D -meson strength being spread out over energies.

In Fig. 4 we display the previous plot of the real and imaginary parts of the s -wave $I = 0$ DN amplitude together with the $I = 1$ channel for a larger energy scale and a smaller range in the y -axis. Apart from the previous three approaches, T-matrix calculation (dotted

lines), in-medium calculation only including Pauli blocking effects (dot-dashed lines) and self-consistent calculation for the D -meson potential (solid lines), we also include the in-medium properties of the nucleons together with the pion self-energy in the self-consistent process for the D -meson potential (long-dashed lines). While the nucleon dressing only shifts the $\Lambda_c(2593)$ resonance in energy, as seen for the $\Lambda(1405)$ resonance, the pion dressing could introduce important changes to the previous self-consistent procedure. In this approach and for $I = 0$, the imaginary part of the DN interaction becomes smoother in the region of energies where the $\Lambda_c(2593)$ resonance was generated in the previous three approaches. For energies below the $\pi\Sigma_c$ threshold, we observe a bump around 2.5 GeV that, in our self-consistent many-body approach, can decay to states such as $\pi(ph)\Sigma_c$ or $D(\Lambda_ch\pi)N$, where in parentheses we have denoted an example for the component of the π and D -meson that show up at energies below $\pi\Sigma_c$. On the other hand, it is also interesting to observe a second structure in the $I = 0$ amplitude, already seen for the three initial approaches, which lies below the DN threshold of 2.806 GeV. This feature in the imaginary part around 2.75 GeV seems to be enhanced in the full self-consistent procedure. This structure, like the previous one, is also a state with the Λ_c -like quantum numbers and, in this case, it can decay to the $\pi\Sigma_c$ state. Whether the first resonant structure is the in-medium $\Lambda_c(2593)$ resonance and the second bump is a new resonance is something that deserves further studies. Note that the energy region of interest for the calculation of the D -meson potential for $I = 0$ lies on the right-hand side of the free $\Lambda_c(2593)$ resonance where this second structure shows up for all approaches. Actually, this is a different feature of the DN interaction compared to the case of the $\bar{K}N$ interaction. The $\bar{K}N$ interaction was basically determined by the behaviour of the s-wave $I = 0$ $\Lambda(1405)$ resonance in the medium. For the $I = 1$ component of the DN interaction, the self-consistent calculation tends to dilute any structure present in the T-matrix. It is seen that for the full self-consistent calculation, the $I = 1$ component is considerably reduced. A more detailed analysis concerning the DN interaction and, hence, the D -meson potential is presented in the following plots.

In Fig. 5 we plot the real and imaginary parts of the D -meson potential at $k_D = 0$ as a function of density for $\Lambda = 1$ GeV and $g^2 = 13.4$ and for the three previous in-medium calculations: in-medium calculation with only Pauli blocking (dot-dashed lines), self-consistent calculation for the D -meson (solid lines) and self-consistent calculation for the D -meson including the dressing of nucleons and the self-energy of pions (long-dashed lines). The D -meson potential becomes more attractive as we increase the density in all three approaches, showing a less smooth behaviour in the case when nucleons and pions are dressed both in the real and imaginary parts. However, the potential turns out to be more attractive for a self-consistent calculation with respect to the case when only Pauli blocking is considered. If we compare these results to the case of the \bar{K} potential, the picture depicted here is different. For the \bar{K} meson case, the shift of the $\Lambda(1405)$ resonance in energy due to the Pauli blocking changes the $\bar{K}N$ scattering amplitude at the threshold from being repulsive to attractive giving rise to an attractive \bar{K} potential. However, when the properties of \bar{K} were incorporated self-consistently, the attraction was drastically reduced [35,41,42]. For the D -meson, the DN threshold is 2.806 GeV and, therefore, the DN amplitude is studied for energies on the right-hand side of the free $\Lambda_c(2593)$ resonance, away from this resonant structure. Furthermore, in the \bar{K} meson case, the s-wave $I = 0$ $\bar{K}N$ amplitude turns out to be the main contribution to the \bar{K} potential due to the presence of the $\Lambda(1405)$ resonance.

For the D -meson, as the energy region of interest is not sitting on the resonance, the $I = 1$ could also become important in the calculation of the D -meson potential.

In order to study the isospin dependence of in-medium DN interaction in more detail as well as the dependence on the chosen set of coupling constants and cutoffs, in Fig. 6 and 7 we represent the real and imaginary parts of the DN amplitude at $\rho = \rho_0$ in the $I = 0$ and $I = 1$ channels as functions of the center-of-mass energy around the DN threshold at total momentum $|\vec{k}_D + \vec{k}_N| = 0$ for the self-consistent calculation when only the D -meson is dressed (Fig. 6) and for the full self-consistent calculation (Fig. 7). Furthermore, in Fig. 8 we show the real and imaginary parts of the D -meson potential at $k_D = 0$ as a function of the density for $\Lambda = 1$ GeV and $g^2 = 13.4$ including the isospin decomposition.

For the first self-consistent approach where only D -mesons are dressed at $\rho = \rho_0$ (Fig. 6), the real parts of the $I = 0$ and $I = 1$ components turn out to be of the same order of magnitude. Therefore, it is not clear which isospin will determine the behaviour of the D -meson potential. Actually, the potential depends on the exact value of both contributions taking into account the isospin factor $2I + 1$ for each isospin component (see Eq. (9)). For $\Lambda = 1$ GeV, the main contribution for the potential at $\rho = \rho_0$ comes from the $I = 1$ component, as seen in Fig. 8. On the other hand, we note that for $\Lambda = 0.8$ GeV, the $I = 0$ component moves from attraction to repulsion as the energy increases (Fig. 6). Nevertheless, the region of integration to obtain the D -meson potential for all the sets of parameters of coupling constants and cutoffs lies around 2.80-2.84 GeV at $\rho = \rho_0$ and, therefore, we obtain a repulsive effect for $I = 0$ and an attractive effect for $I = 1$ in the potential at $\rho = \rho_0$ for all sets (see Fig. 8 for $\Lambda = 1$ GeV). The imaginary part displays a smoother behaviour than in the case of the full self-consistent calculation. When the full calculation is performed (Fig. 7), the peak observed around energies of 2.75 GeV gets diluted with increasing cutoff. However, the real part shows more structure than in the previous self-consistent approach and the $I = 0$ component becomes more important with respect to the previous case. This effect together with a less important contribution of the $I = 1$ component makes the $I = 0$ govern the D -meson potential for densities larger than $\rho = 1.5\rho_0$ for all sets. For $\rho = \rho_0$ and $\Lambda = 1$ GeV, the attractive $I = 1$ component still dominates. What it is not so clear is whether the $I = 0$ will be attractive or repulsive for all the sets as the region of integration lies around 2.71-2.78, where the $I = 0$ real part changes in sign. The different region of the integration in this last case with respect to the case where only the D -meson is dressed is mainly due to the inclusion of an attractive potential for the nucleons as the value of the D -meson potential does not change by a great amount for both self-consistent processes (see Fig. 8).

In Fig. 8 we observe that, in the case where only the D -meson is dressed and for $\Lambda = 1$ GeV, the real part of the D -meson potential is governed by the $I = 1$ component as density grows. This is also seen for the other set of parameters studied. On the other hand, for the full calculation, the $I = 0$ component controls the behaviour of the D -meson potential as we increase the density not only for $\Lambda = 1$ GeV but also for the other sets. This is due to the resonant structure seen in Fig. 7 that also causes a less smooth behaviour of the D -meson potential.

In order to study the dependence on the cutoff and coupling constant, we show in Fig. 9 the D -meson potential at $k_D = 0$ as a function of the density for different sets of coupling constants and cutoffs and for the two approaches mentioned before. When only the D -meson

is dressed, higher densities are required in order to obtain an attractive potential with respect to the full self-consistent calculation. In both cases, the D -meson potential tends to get more attractive as density increases. The reason is that, in order to obtain the D -meson potential as density increases, we are integrating over a larger energy region where the interaction is attractive. However, as mentioned in the previous plot, the isospin component responsible for that behaviour is different depending on the approach. On the other hand, the value of the potential turns out to be slightly sensitive to the chosen set of parameters. There is, however, in both cases a density for which all sets give the same value for the D -meson potential. When only the D -meson is dressed, we obtain a range of values for the D -meson potential at $\rho = \rho_0$ between 8.6 MeV for $\Lambda = 0.8$ GeV and -11.2 MeV for $\Lambda = 1.4$ GeV. For the full self-consistent calculation, the range of values covered lies in between 2.6 MeV for $\Lambda = 0.8$ GeV and -12.3 MeV for $\Lambda = 1.4$ GeV. This result would indicate that our self-consistent coupled-channel calculation gives a different prediction for the D -meson potential as compared to the calculations based on the QCD sum-rule approach [16,19], the quark-meson coupling model [21], lattice calculations [20,31,32] and a recent work based on a chiral model that obtains the medium modification of the mass of D-meson due to its interaction with the light hadron sector [33]. The calculations based on the QCD sum rule approach as well as quark-meson coupling model predict the mass drop of the D-meson to be of the order of 50-60 MeV at nuclear matter density. A similar drop at finite temperatures [20] is suggested from the lattice calculations for heavy quark potentials. An interaction Lagrangian based on chiral perturbation theory also gives a similar shift at nuclear matter density, when the Tomozawa-Weinberg interaction is supplemented by the attractive DN Sigma term and the charm content of the nucleon is ignored [33]. On the other hand, the effective chiral Lagrangian approach [33] is seen to yield a larger drop of the D-meson masses ($\simeq 200$ MeV at nuclear matter density). In the present calculation, the coupled-channel effects seem to result in an overall drastic reduction of the in-medium effects independent of the parameters (g, Λ) and the in-medium properties of the intermediate states compared to the previous works.

Finally, once self-consistency is reached, we calculate the full energy dependence of the D -meson self-energy which defines the in-medium D -meson single-particle propagator and its spectral density (see Eqs. (13-14)). The spectral density at zero momentum is shown in Fig. 10 for $\Lambda = 1$ GeV and for several densities in the two approaches considered before. In the case when only the D -meson is dressed in the self-consistent process, the peak of the D -meson pole moves towards lower energies as density increases since the D -meson potential becomes more attractive for $\Lambda = 1$ GeV (see Fig. 9). Moreover, it is observed that the D -meson spectral density falls off more slowly on the left-hand side of the quasiparticle peak as density increases. This is due to the $I = 1$ component of the off-shell D -meson self-energy, which is related to the D -meson potential through Eq. (12). As density increases, we have already discussed that the $I = 1$ component governs the behaviour of the potential and, hence, the self-energy. Therefore, any structure lying close the quasiparticle peak is enhanced and clearly visible in the spectral density. On the other hand, we also notice some structure of the spectral density to the left of the quasiparticle peak at energies of the D -meson of around 1.63-1.65 GeV, the origin of which could be traced back to the presence of the $\Lambda_c(2593)$ resonance.

For the full self-consistent calculation, the quasiparticle peak moves towards lower ener-

gies as density increases according to the behaviour of the D -meson potential seen in Fig. 9, although there is region of densities around $0.5\rho_0$ where the D -meson potential turns out to be repulsive. For densities between ρ_0 and $1.5\rho_0$, the quasiparticle peak mixes with a structure, already noticed on the left-hand side of the quasiparticle peak for $0.5\rho_0$, making it more difficult to separate the contribution of the quasiparticle peak and the effect of this structure. This bump in the spectral density is due to the structure observed in the imaginary part of the $I = 0$ component of the in-medium DN interaction which lies close to the DN threshold. The nature of this structure and in-medium changes of the D -meson production could probably be studied experimentally in the near future with the PANDA experiment at the GSI International Facility in Darmstadt [45].

IV. CONCLUSIONS

We have performed a microscopic self-consistent coupled-channel calculation of the single-particle potential of the D -meson and, hence the D -meson spectral density, embedded in symmetric nuclear matter assuming a separable potential for the s-wave DN interaction.

The $\Lambda_c(2593)$ resonance, which is the counterpart of the $\Lambda(1405)$ in the charm sector, has been generated dynamically for a given set of coupling constants g and cutoffs Λ .

We have also studied the medium effects on the $\Lambda_c(2593)$ resonance and, hence on the D -meson potential, due to the Pauli blocking of the intermediate nucleonic states as well as due to the dressing of nucleons and pions. The D -meson optical potential has been obtained for different approaches: in-medium calculation including only Pauli blocking on the intermediate nucleonic states, self-consistent calculation for the D -meson and self-consistent calculation for the D -meson including the dressing of nucleons and the pion self-energy.

We observe that the two self-consistent schemes show a stronger density dependence compared to the case when only Pauli blocking effects are included. When only the D -meson is dressed in the self-consistent procedure, the D -meson potential at $\rho = \rho_0$ stays between 8.6 MeV for $\Lambda = 0.8$ GeV and -11.2 MeV for $\Lambda = 1.4$ GeV. For the full self-consistent calculation, the range of values covered lies in between 2.6 MeV for $\Lambda = 0.8$ GeV and -12.3 MeV for $\Lambda = 1.4$ GeV. We conclude that the coupled-channel effects seem to result in an overall reduction of the in-medium effects independent of the set of parameters (g, Λ) and the in-medium properties of the intermediate states compared to previous work.

The isospin dependence of the D -meson in both approaches have been also analyzed. While the $I = 1$ amplitude governs the behaviour of the D -meson potential when only D -mesons are dressed, the D -meson is basically determined by the $I = 0$ component in the full self-consistent calculation.

The D -meson spectral density has been finally obtained for both self-consistent schemes. Although the quasiparticle peak stays closer to its free position in both cases for nuclear matter saturation density, the features of the low-energy region on the left-hand side of the quasiparticle peak are different according to the different in-medium behaviour of the $\Lambda_c(2593)$ resonance in both approaches.

The in-medium effects devised in this work can be studied in heavy-ion experiments at the future International Facility at GSI. The PANDA experiment at GSI [45] will measure hadrons with charm by antiproton beams on nuclei with its microvertex detector. In-medium changes of open charm hadrons can be addressed by the study of the excitation function

and the correlation function of D - and \bar{D} -mesons. We stress that, although the in-medium potential for D -mesons has turned out to be quite small in our investigation, the production of D -meson in the nuclear medium will be still enhanced due to the additional strength of the D -meson spectral function below the quasiparticlepeak. This effect is similar to the one extracted for the enhanced \bar{K} production in heavy-ion collisions [46].

The present coupled-channel approach to the D -meson properties in the nuclear medium is, as the first of its kind, exploratory and can be improved by incorporating relativistic potentials as well as chiral constraints on the bare hadronic interactions. It will be also interesting to explore the in-medium effects for D -mesons in dynamical approaches for studying e.g. the excitation function, which we will leave for future work.

ACKNOWLEDGMENTS

The authors are very grateful to A. Ramos for critical reading of the manuscript. L.T. wishes to acknowledge the financial support from the Alexander von Humboldt Foundation. A.M. is grateful to the Institut für Theoretische Physik for warm hospitality and acknowledges financial support from Bundesministerium für Bildung and Forschung (BMBF).

REFERENCES

- [1] G. Agakichiev *et al.*, CERES collaboration, Phys. Rev. Lett. **75**, 1272 (1995); G. Agakichiev *et al.*, CERES collaboration, Phys. Lett. B **422**, 405 (1998); G. Agakichiev *et al.*, CERES collaboration, Nucl. Phys. **A661**, 23c (1999).
- [2] N. Masera *et al.*, HELIOS-3 collaboration, Nucl. Phys. **A590**, 93c (1995).
- [3] E. L. Bratkovskaya and W. Cassing, Nucl. Phys. **A619**, 413 (1997).
- [4] W. Cassing and E. L. Bratkovskaya, Phys. Rep. **308**, 65 (1999).
- [5] A. Mishra, J. C. Parikh and W. Greiner, J. Phys. G **28**, 151 (2002).
- [6] A. Mishra, J. Reinhardt, H. Stöcker and W. Greiner, Phys. Rev. C **66**, 064902 (2002).
- [7] G. Q. Li, C. M. Ko and G. E. Brown, Nucl. Phys. **A606**, 568 (1996).
- [8] C. M. Ko, J. Phys. G **27**, 327 (2001).
- [9] G. Q. Li, C.-H. Lee and G. E. Brown, Nucl. Phys. **A625**, 372 (1997).
- [10] S. Pal, C. M. Ko, and Z.-W. Lin, Phys. Rev. C **64**, 042201 (2001).
- [11] F. Laue *et al.*, Phys. Rev. Lett. **82**, 1640 (1999).
- [12] C. Sturm *et al.*, Phys. Rev. Lett. **86**, 39 (2001).
- [13] A. Förster *et al.*, KaoS Collaboration, J. Phys. G **28**, 2011 (2002).
- [14] M. Menzel *et al.*, Phys. Lett. B **495**, 26 (2000).
- [15] W. Cassing, L. Tolós, E. L. Bratkovskaya, A. Ramos, Nucl. Phys. **A727**, 59 (2003).
- [16] A. Hayashigaki, Phys. Lett. B **487**, 96 (2000).
- [17] W. Liu, C. M. Ko and Z. W. Lin, Phys. Rev. C **65**, 015203 (2001).
- [18] B. Friman, S. H. Lee and T. Song, Phys. Lett. B **548**, 153 (2002).
- [19] P. Morath, W. Weise and S. H. Lee, *Proceedings of the 17th Autumn school on QCD: Perturbative or Nonperturbative?* Lisbon 1999, edited by L. S. Ferreira, P. Nogueira, and J. I. Silva-Marcos (World Scientific, Singapore, 2001), p. 425
- [20] S. Digal, P. Petreczky and H. Satz, Phys. Lett. B **514**, 57 (2001).
- [21] K. Tsushima, D. H. Lu, A. W. Thomas, K. Saito, and R. H. Landau, Phys. Rev. C **59**, 2824 (1999); A. Sibirtsev, K. Tsushima, and A. W. Thomas, Eur. Phys. J. A **6**, 351 (1999).
- [22] W. Cassing, E. L. Bratkovskaya, and A. Sibirtsev, Nucl. Phys. **A691**, 753 (2001).
- [23] M. Gonin *et al.*, NA50 Collaboration, Nucl. Phys. **A610**, 404c (1996).
- [24] M. C. Abreu *et al.*, NA50 Collaboration, Eur. Phys. J. C **14**, 443 (2000).
- [25] Z. Lin and C. M. Ko, J. Phys. G **27**, 617 (2001).
- [26] K. Adcox *et al.*, Phys. Rev. Lett. **88**, 192303 (2002).
- [27] J. P. Blaizot and J. Y. Ollitrault, Phys. Rev. Lett. **77**, 1703 (1996).
- [28] B. Zhang, C. M. Ko, B. A. Li, Z. Lin, and B. H. Sa, Phys. Rev. C **62**, 054905 (2000).
- [29] W. Cassing and E. L. Bratkovskaya, Nucl. Phys. **A623**, 570 (1997).
- [30] E. L. Bratkovskaya, W. Cassing and H. Stöcker, Phys. Rev. C **67**, 054905 (2003).
- [31] C. Y. Wong T. Barnes, E. S. Swanson and H. W. Crater, nucl-th/0112023.
- [32] F. Karsch, E. Laermann and A. Peikert, hep-lat/0012023; F. Karsch *et al.*, Nucl. Phys. B **502**, 321 (2001).
- [33] A. Mishra, E. L. Bratkovskaya, J. Schaffner-Bielich, S. Schramm and H. Stöcker, Phys. Rev. C **69**, 015202 (2004).
- [34] A. Mishra, K. Balazs, D. Zschesche, S. Schramm, H. Stöcker, and W. Greiner, Phys. Rev. C **69**, 024903 (2004).
- [35] L. Tolós, A. Ramos, A. Polls, and T.T.S. Kuo, Nucl. Phys. **A690**, 547 (2001).

- [36] V. Koch, Phys. Lett. B **337**, 7 (1994).
- [37] P. B. Siegel, and W. Weise, Phys. Rev. **C38**, 2221 (1998).
- [38] L. Tolós, A. Ramos, and A. Polls, Phys. Rev. **C65**, 054907 (2002).
- [39] R. Machleidt, Adv. Nucl. Phys. **19**, 189 (1989).
- [40] A. L. Fetter, and J. D. Walecka, *Quantum Theory of Many-Particle Systems* (International Series in Pure and Applied Physics, Mc Graw-Hill, NY, USA, 1971); T. E. Ericsson, and W. Weise, *The international Series of Monographs on Physics*, 74 (Clarendon, Oxford, UK, 1998), 479 p; E. Oset, *Proceedings: Quarks, Mesons and Isobars in Nuclei*, Motril, 1-60 (1982).
- [41] A. Ramos, and E. Oset, Nucl. Phys. **A671**, 481 (2000).
- [42] M. Lutz, Phys. Lett. B **426**, 12 (1998).
- [43] M. F. M. Lutz, and E. E. Kolomeitsev, Nucl. Phys. **A730**, 110 (2004).
- [44] T. Waas, N. Kaiser, and W. Weise, Phys. Lett. B **365**, 12 (1996); T. Waas, N. Kaiser, and W. Weise, Phys. Lett. B **379**, 34 (1996); T. Waas, and W. Weise, Nucl. Phys. **A625**, 287 (1997).
- [45] J. Ritman, Eur. Phys. J. A **18**, 177 (2003); Nucl. Instrum. Meth. B **214**, 201 (2004), and private communication
- [46] L. Tolós, A. Polls, A. Ramos and J. Schaffner-Bielich, Phys. Rev. **C68**, 024903 (2003).

FIGURES

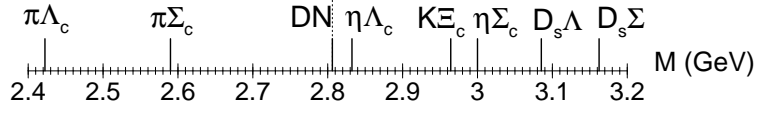


FIG. 1. Mass thresholds

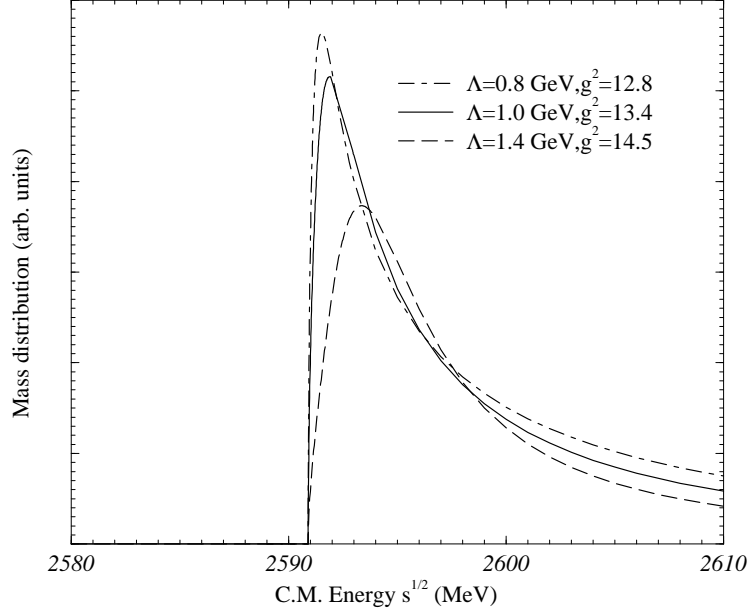


FIG. 2. $\Lambda_c(2593)$ mass spectrum for different sets of coupling constants and cutoffs.

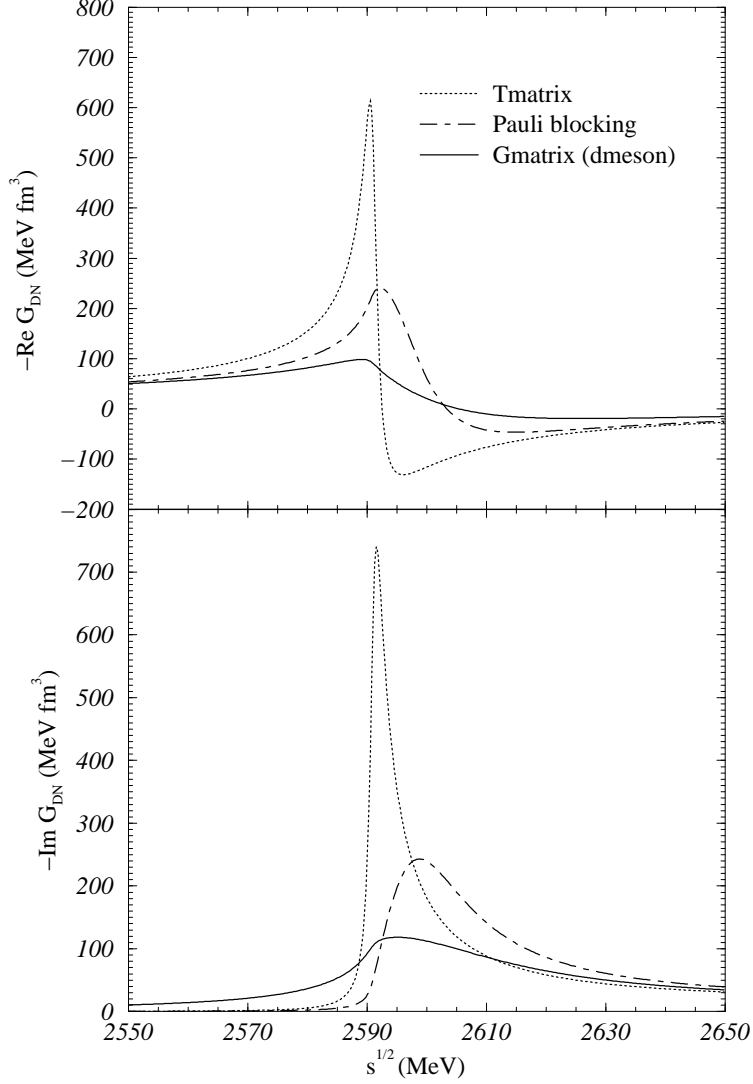


FIG. 3. Real and imaginary parts of the s-wave DN amplitude in the $I = 0$ channel as functions of the center-of-mass energy at total momentum $|\vec{k}_D + \vec{k}_N| = 0$ for $\Lambda = 1$ GeV and $g^2 = 13.4$ and for different approaches: T-matrix calculation (dotted lines), in-medium calculation including only Pauli blocking at $\rho = \rho_0$ (dot-dashed lines) and self-consistent calculation for the D -meson at $\rho = \rho_0$ (solid lines).

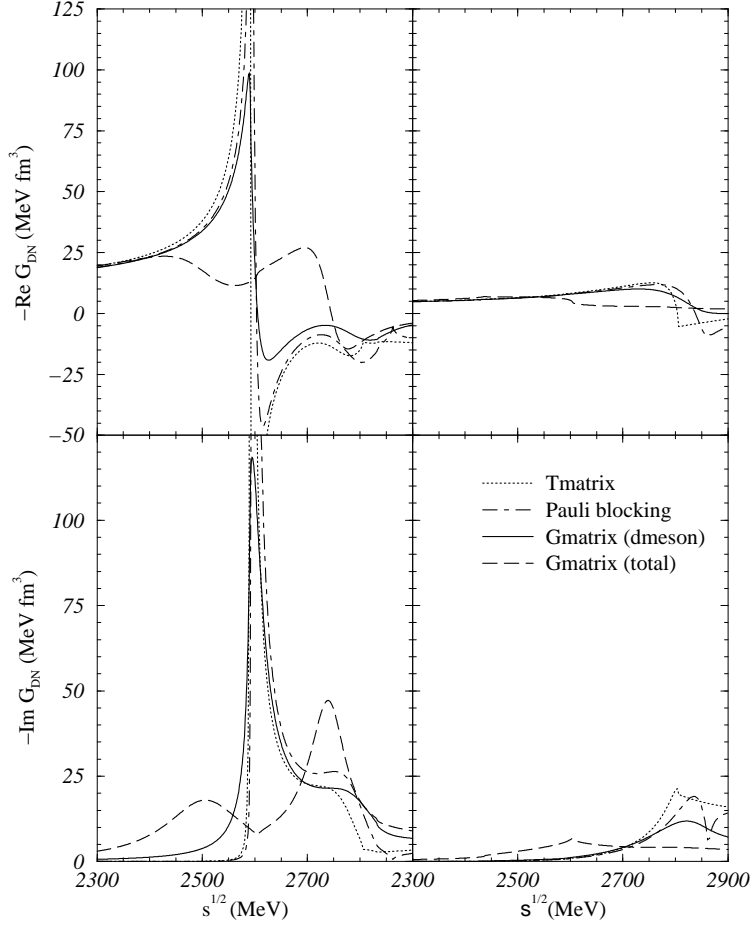


FIG. 4. Real and imaginary parts of the s-wave DN amplitude in the $I = 0$ channel (left panels) and $I = 1$ channel (right panels) as functions of the center-of-mass energy at total momentum $|\vec{k}_D + \vec{k}_N| = 0$ in a larger scale of energy for $\Lambda = 1$ GeV and $g^2 = 13.4$ and for different approaches: T-matrix calculation (dotted lines), in-medium calculation including only Pauli blocking at $\rho = \rho_0$ (dot-dashed lines), self-consistent calculation for the D -meson at $\rho = \rho_0$ (solid lines) and self-consistent calculation for the D -meson including the dressing of nucleons and the pion self-energy at $\rho = \rho_0$ (long-dashed lines).

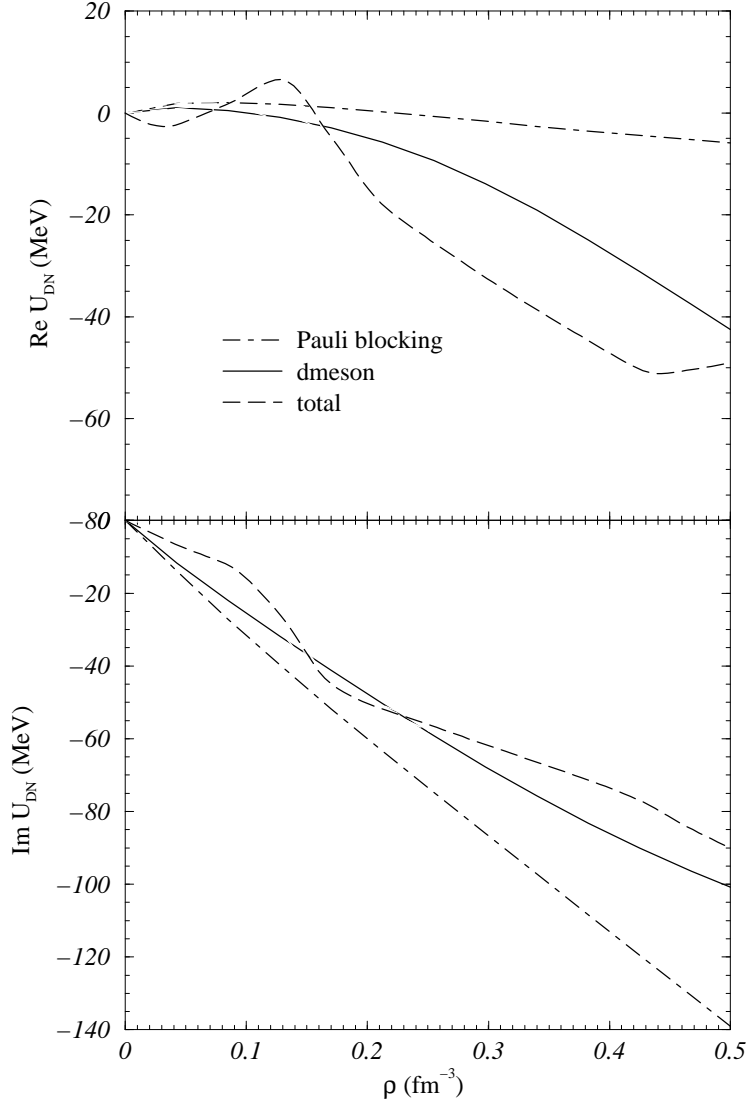


FIG. 5. Real and imaginary parts of the D -meson potential at $k_D = 0$ as a function of density for $\Lambda = 1$ GeV and $g^2 = 13.4$ and for different approaches: in-medium calculation including only Pauli blocking (dot-dashed lines), self-consistent calculation for the D -meson (solid lines) and self-consistent calculation for the D -meson including the dressing of nucleons and the pion self-energy (long-dashed lines).

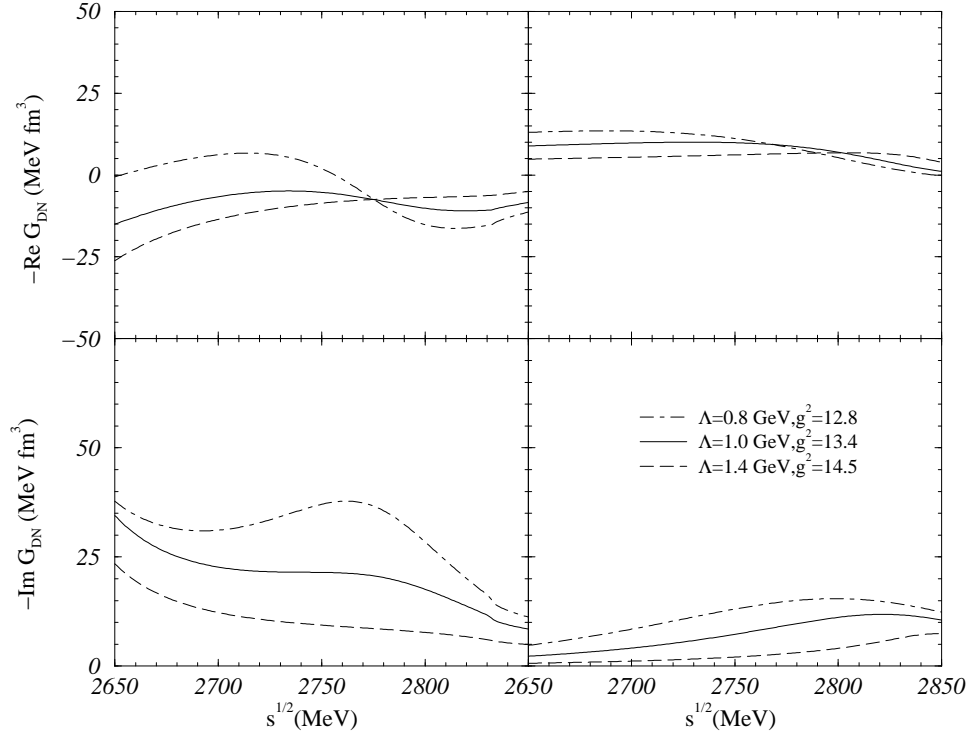


FIG. 6. Real and imaginary parts of the s-wave DN amplitude at $\rho = \rho_0$ in the $I = 0$ (left panels) and $I = 1$ (right panels) channels as functions of the center-of-mass energy at total momentum $|\vec{k}_D + \vec{k}_N| = 0$ for the self-consistent calculation for the D -meson and for different sets of coupling constants and cutoffs.

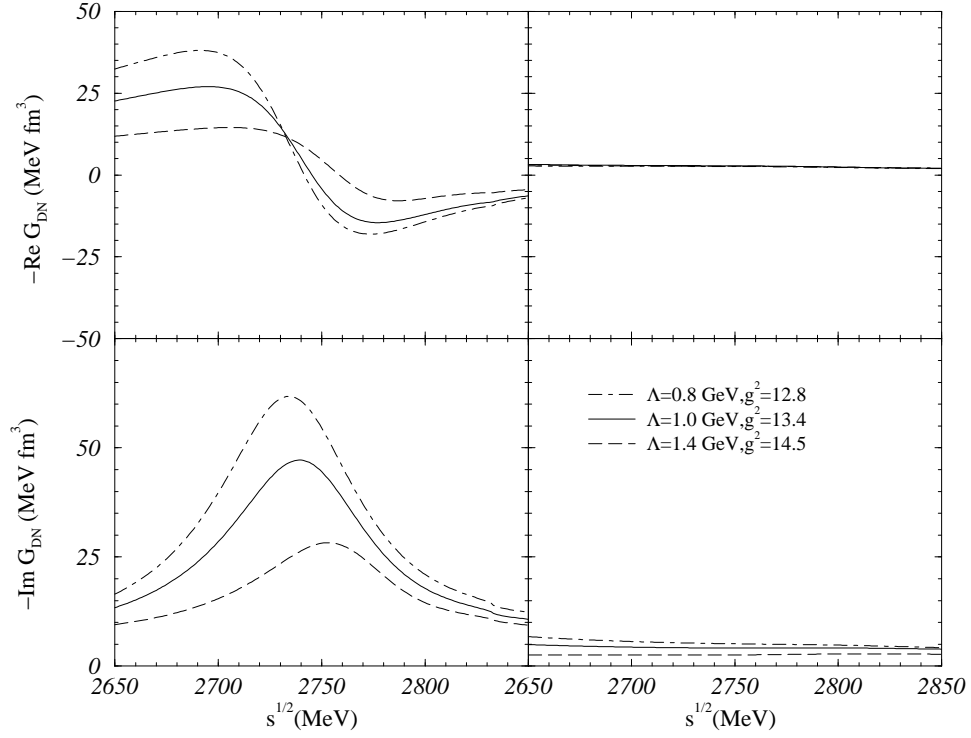


FIG. 7. Real and imaginary parts of the DN amplitude at $\rho = \rho_0$ in the $I = 0$ (left panels) and $I = 1$ (right panels) channels as functions of the center-of-mass energy at total momentum $|\vec{k}_D + \vec{k}_N| = 0$ for the self-consistent calculation for the D -meson including the dressing of nucleons and the pion self-energy and for different sets of coupling constants and cutoffs.

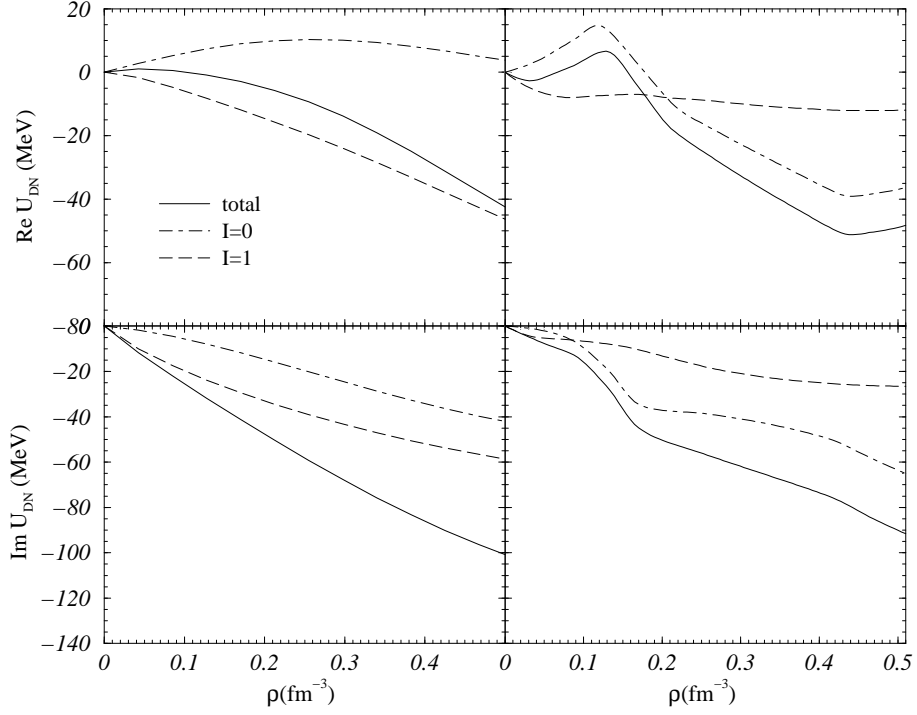


FIG. 8. Real and imaginary parts of the D -meson potential at $k_D = 0$ as a function of the density for $\Lambda = 1$ GeV and $g^2 = 13.4$ including the isospin decomposition for two approaches: self-consistent calculation for the D -meson (left panels) and self-consistent calculation for the D -meson including the dressing of nucleons and the pion self-energy (right panels).

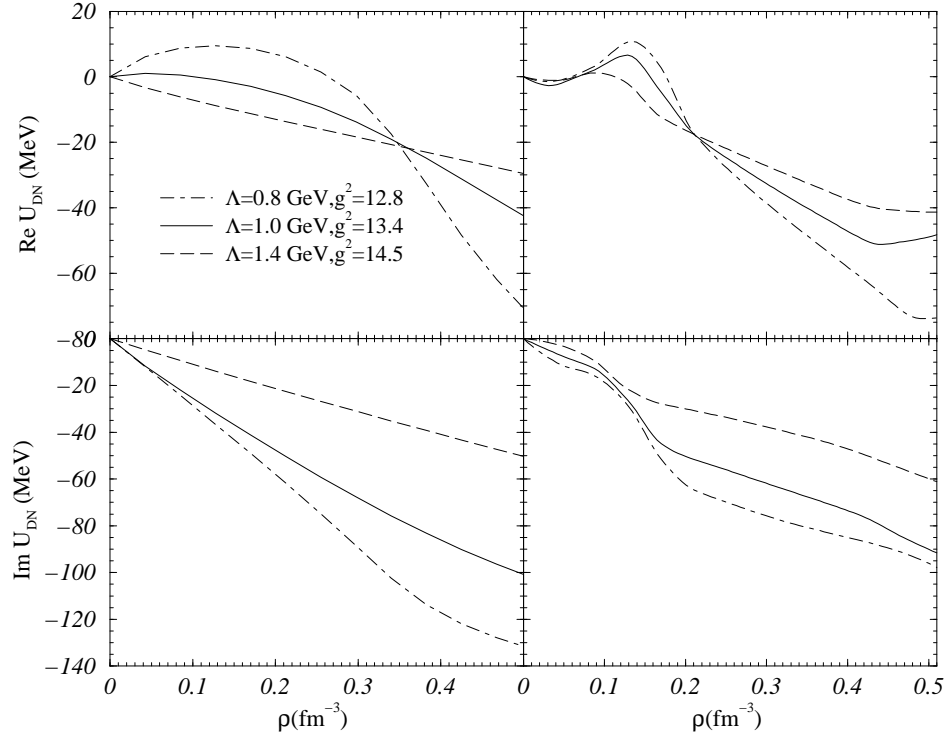


FIG. 9. Real and imaginary parts of the D -meson potential at $k_D = 0$ as a function of the density for different sets of coupling constants and cutoffs and for two approaches: self-consistent calculation for the D -meson (left panels) and self-consistent calculation for the D -meson including the dressing of nucleons and the pion self-energy (right panels).

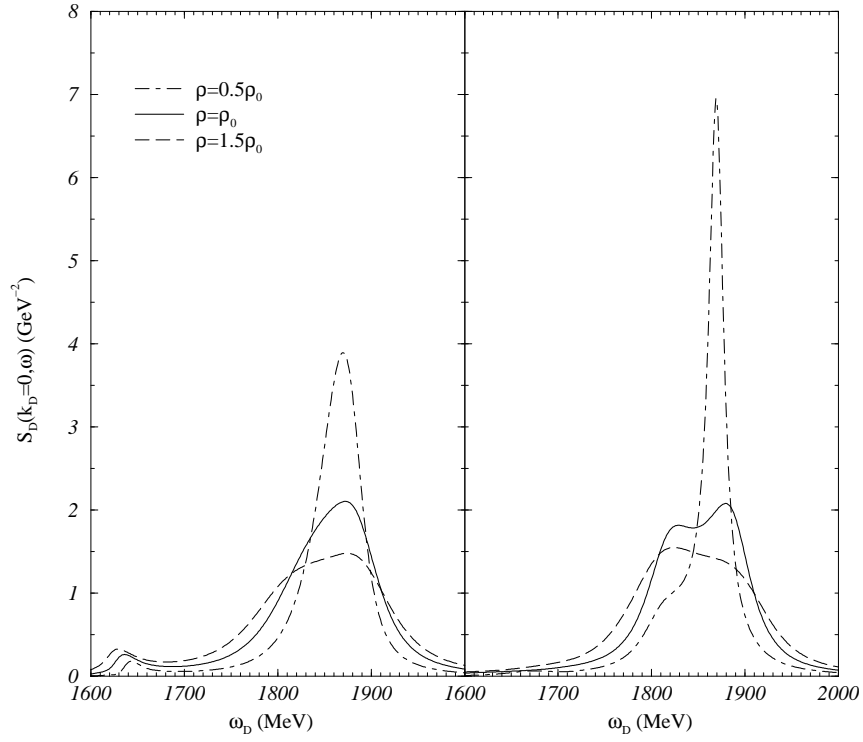


FIG. 10. D -meson spectral density at $k_D = 0$ as a function of energy with $\Lambda = 1$ GeV and $g^2 = 13.4$ for different densities and for two approaches: self-consistent calculation for the D -meson (left panels) and self-consistent calculation for the D -meson including the dressing of nucleons and the pion self-energy (right panels).